

The Structure of the Free MnF₃ Molecule—A Beautiful Example of the Jahn–Teller Effect

Magdolna Hargittai,^{*,†,‡} Balázs Réffy,[§] Mária Kolonits,[†] Colin J. Marsden,^{*,⊥} and Jean-Louis Heully[⊥]

Contribution from the Structural Chemistry Research Group of the Hungarian Academy of Sciences, Eötvös University, Pf. 117, H-1431 Budapest, Hungary, Institute of General and Analytical Chemistry, Budapest Technical University, H-1521 Budapest, Hungary, and IRSAMC, Laboratoire de Physique Quantique CNRS UMR 5626, Université Paul Sabatier, 118 route de Narbonne, 31062 Toulouse Cedex, France

Received April 16, 1997[⊗]

Abstract: A new high-temperature gas-phase electron diffraction analysis of manganese trifluoride, combined with high-level quantum chemical calculations, provides direct geometrical evidence of a Jahn–Teller distortion in a free molecule. The potential energy surface of the molecule was scanned extensively by computation at the SCF level. CASSCF and CASPT2 calculations established that of the many C_{2v} symmetry stationary points on the potential energy surface the lowest energy ones are quintets. The global minimum is a quintet state of 5A_1 symmetry. In this planar C_{2v} symmetry structure there are two longer and one somewhat shorter Mn–F bonds, with two bond angles close to 106° and one bond angle of about 148° . The second lowest energy state was of 5B_2 symmetry, which turned out to be a transition state with an imaginary b_2 (in plane) bending frequency. A constrained planar structure of D_{3h} molecular symmetry has appreciably higher energy than the 5B_2 symmetry structure. The experimental data are in complete agreement with the results of the computations in giving the best agreement with a C_{2v} structure characterized by $r_g(\text{Mn–F}) = 1.728 \pm 0.014 \text{ \AA}$ (once), $r_g(\text{Mn–F}) = 1.754 \pm 0.008 \text{ \AA}$ (twice), $\angle_\alpha(\text{F–Mn–F}) = 106.4 \pm 0.9^\circ$ (twice), and $\angle_\alpha(\text{F–Mn–F}) = 143.3 \pm 2.0^\circ$ (once). Our computed infrared wavenumbers and intensities make an assignment possible for published vibrational spectra of MnF₃.

Introduction

The Jahn–Teller effect is one of the truly subtle effects in structural chemistry. According to its original formulation,¹ a nonlinear, symmetric molecule with an orbitally degenerate electronic state is unstable and gets distorted, thereby removing the electronic degeneracy, until a nondegenerate ground state is achieved. The effect involves the coupling of the electronic and vibrational motions of the molecule. The ground state orbital degeneracy is removed by distorting the highly symmetrical geometry to a lower symmetry structure. Only those types of vibration are capable of doing so whose symmetry matches the symmetry of the electronic state: they have to belong to the same irreducible representation of the molecular point group as one of the irreducible representations that the direct product of the symmetry of the ground state with itself reduces to.^{2–4}

Only certain systems are subjects to Jahn–Teller distortion depending, inter alia, on the number and spin state of their valence electrons and their coordination number. Octahedral d^4 and d^9 transition metal complexes are typical examples. Manganese trifluoride has always been considered a prototype

“Jahn–Teller system” together with chromium and copper dihalides. Indeed, the crystals of these systems, all MX_6 octahedral types, show considerable tetragonal distortion.⁵ A recent X-ray crystallography study⁶ of manganese trifluoride confirmed the results of earlier work,⁷ in that the MnF₃ crystals have a distorted octahedral shape. There are four Mn–F distances close to each other and two that are much longer, thus there is a tetragonal elongation of the octahedron in the crystal and a decrease of symmetry from O_h to D_{4h} .

There is no a priori reason that the Jahn–Teller effect should occur only in crystals. Such distortions should be possible in free, gas-phase molecules, provided that they have a degenerate ground electronic state. In the electron diffraction studies of CrF₅⁸ and MoCl₅⁹ deviations from D_{3h} symmetry were observed and were attributed to a dynamic Jahn–Teller effect, although this could not be unambiguously confirmed in either investigation. A recent density functional study¹⁰ supports the idea of dynamical Jahn–Teller effect in CrF₅.

Nonetheless, to our knowledge, direct experimental evidence has never been found for the Jahn–Teller effect in a free gas-phase molecule. One of the reasons for a lack of such data could be that transition metal dihalides, such as CrX₂ and CuX₂, which are the most typical Jahn–Teller systems in the crystal phase, are linear molecules in the gas phase and thus the Jahn–

* To whom correspondence should be addressed. E-mail: hargittaim@ludens.elte.hu.

† Eötvös University.

‡ 1996/97 academic year at the University of North Carolina at Wilmington, Wilmington, NC 28403.

§ Budapest Technical University.

⊥ Université Paul Sabatier.

⊗ Abstract published in *Advance ACS Abstracts*, August 15, 1997.

(1) Jahn, H. A.; Teller, E. *Proc. R. Soc. London, Ser. A* **1937**, *161*, 220.

(2) Hargittai, I.; Hargittai, M. *Symmetry through the Eyes of a Chemist*, 2nd ed.; Plenum Press: New York, 1995.

(3) Pearson, R. G. *Symmetry Rules for Chemical Reactions: Orbital Topology and Elementary Processes*; Wiley-Interscience: New York, 1976.

(4) Bersuker, I. B. *The Jahn–Teller Effect and Vibronic Interactions in Modern Chemistry*; Plenum Press: New York, 1984.

(5) Wells, A. F. *Structural Inorganic Chemistry*, 4th ed.; Clarendon Press: Oxford, 1975.

(6) Schrötter, F.; Müller, B. G. *Z. Anorg. Allg. Chem.* **1993**, *619*, 1426.

(7) Hepworth, M. A.; Jack, K. H. *Acta Crystallogr.* **1957**, *10*, 345.

(8) Jacob, E. J.; Hedberg, L.; Hedberg, K.; Davis, H.; Gard, G. L. *J. Phys. Chem.* **1984**, *88*, 1935.

(9) Faegri, K.; Martinsen, K.-G.; Strand, T. G.; Volden, H. V. *Acta Chem. Scand.* **1993**, *47*, 547.

(10) Vanquickenborne, L. G.; Vinckier, A. E.; Pierloot, K. *Inorg. Chem.* **1996**, *35*, 1305.

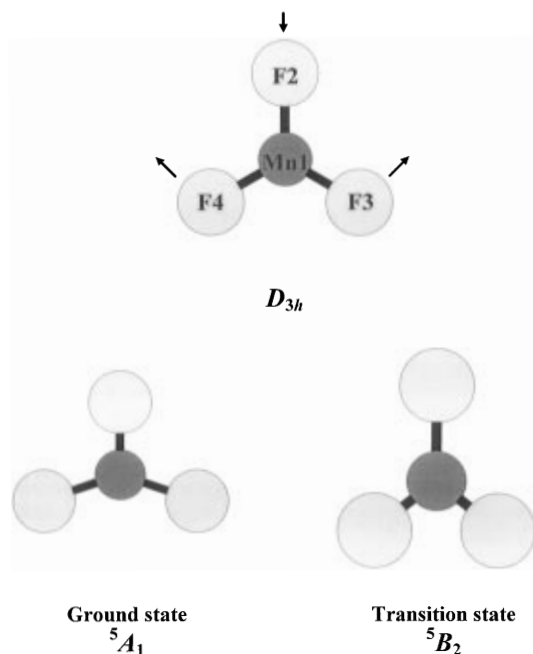


Figure 1. The expected Jahn–Teller-type deformation of the trigonal planar manganese trifluoride molecule. Both ground-state and transition-state geometries, with C_{2v} symmetry, are indicated.

Teller effect does not apply to them. Manganese trifluoride, on the other hand, is an ideal candidate for observing this effect.

Supposing that MnF₃ has a planar, D_{3h} symmetry structure, as other transition metal trihalides, such as CrF₃¹¹ and FeF₃,¹² do, the symmetry of its ground electronic state could be ${}^5E'$ as was discussed in an early quantum chemical study by Yates and Pitzer.¹³ Such a molecule would qualify for a Jahn–Teller distortion, but computational difficulties did not allow them to investigate lower symmetry structures at that time.

Considering the symmetry of the ground state of a planar MnF₃ molecule and the possible normal modes of vibrations of such a molecule, it is an e' type vibration that can lower the symmetry of the molecule and stabilize it.¹⁴ This means an in-plane deformation of the molecule into a C_{2v} symmetry shape (see Figure 1). This is the only normal mode that has the right symmetry for the distortion. This also means that we cannot expect the molecule to decrease its symmetry toward a C_{3v} symmetry structure since that would involve an out-of-plane vibration, with a_2'' symmetry, but there is no irreducible representation with a_2'' symmetry among the irreducible representations that the direct product of e' with itself reduces to. Therefore, C_{3v} -type distortion does not seem to be possible, at least not in the Jahn–Teller manner.

Manganese trifluoride was investigated by electron diffraction recently by Girichev et al.¹⁵ They found two models of the MnF₃ molecule to approximate equally well their electron diffraction data, viz., a C_{3v} and a Jahn–Teller distorted C_{2v} structure. They also concluded that the C_{3v} symmetry geometry could not be a consequence of out-of-plane distortions of a D_{3h} planar equilibrium configuration because such an assignment

would imply unrealistically large shrinkage effects.¹⁶ Thus, they suggested that the molecule is either pyramidal or planar with C_{2v} symmetry.

We have found the structure of MnF₃ intriguing and, at first, we decided to carry out some quantum chemical calculations to help to distinguish between the two models, C_{3v} and C_{2v} . We then used some of our computational results as constraints in a reanalysis of Dr. Girichev's experimental data which he had kindly sent us. However, even with these constraints it was impossible to make a distinction between his two proposed models.

Since high-temperature electron diffraction experiments present a great challenge, at this point we decided to carry out our own independent electron diffraction experiment. We found it especially important to collect the highest-quality data possible and at the widest possible scattering angle range. While we were working on the analysis, a new matrix-isolation infrared and Raman investigation of MnF₃ appeared in the literature by Bukhmarina and Predtechenskii.¹⁷ Their conclusion was that the molecule must be distorted from a D_{3h} planar configuration. While they strongly suggested that the distortion may be due to the Jahn–Teller effect, they did not give an assignment to their frequencies. Nonetheless, they suggested that their results may be the first direct observation of the Jahn–Teller effect in a vibrational spectrum.

In the present paper we report our electron diffraction investigation of manganese trifluoride together with quantum chemical calculations and normal coordinate analysis based on the experimental¹⁷ and our computed frequencies.

Experimental Section

The electron diffraction patterns of a Sigma-Aldrich MnF₃ sample were recorded in our modified EG-100A apparatus¹⁸ with a high-temperature nozzle system.¹⁹ The nozzle material was nickel. To avoid thermal decomposition the lowest possible temperature and gas pressure were employed, using a special, relatively wide nozzle (\varnothing 0.7 mm) at a nozzle temperature of 1000 K.

The electron diffraction experiments were performed by using 60 kV electrons at two camera ranges, 50 and 19 cm, respectively, using Kodak electron image plates. Five and three photoplates were selected for analysis at the 50 and 19 cm camera range, respectively. The data intervals at the 50 and 19 cm experiments are $s = 2\text{--}14$ (with data steps of 0.125 \AA^{-1}) and $9\text{--}30 \text{ \AA}^{-1}$ (with data steps of 0.25 \AA^{-1}), respectively. Due to the increasing noise level, over $s = 20 \text{ \AA}^{-1}$ at the 19 cm experiment, a diminishing weight was applied to these data. The electron scattering factors were taken from the literature.²⁰ The molecular intensities of MnF₃ are plotted in Figure 2. Listings of the total electron diffraction intensities are available from the authors upon request.

Computational Section

In a zeroth-order approximation, MnF₃ may be regarded as composed of an Mn³⁺ cation and three F[−] anions. Since the ground state valence configuration of an isolated Mn³⁺ ion is $3d^4$, quintet states of MnF₃ must be investigated, while triplet states cannot be excluded without quantitative calculations. If one wishes to compare triplet and quintet states on an equal

(11) Zadorin, E. Z.; Ivanov, A. A.; Ermolaeva, L. I.; Spiridonov, V. P. *Zh. Fiz. Khim.* **1989**, *63*, 669.

(12) Hargittai, I.; Kolonits, M.; Tremmel, J.; Fourquet, F.-L.; Ferey, G. *Struct. Chem.* **1990**, *1*, 75.

(13) Yates, J. H.; Pitzer, R. M. *J. Chem. Phys.* **1979**, *70*, 4049.

(14) For an early detailed treatment of the trigonal case, see: Liehr, A. D. Parts I–III. In *Progress in Inorganic Chemistry*; Cotton, F. A., Ed.; Interscience: New York, London, 1961, 1962, 1966; Vol. 3, 4, 5.

(15) Girichev, G. V.; Giricheva, N. I.; Petrova, V. N.; Shlykov, S. A.; Rakov, E. G. *Zh. Strukt. Khim.* **1994**, *35* (6), 61.

(16) The shrinkage effect in this case would be an apparent shortening of the F...F distances due to the out-of-plane vibrations. See, e.g.: Hargittai, I. In *Stereochemical Applications of Gas-Phase Electron Diffraction*; Hargittai, I., Hargittai, M., Eds.; VCH: New York, 1988; Vol. A, p 1.

(17) Bukhmarina, V. I.; Predtechenskii, Yu. B. *Opt. Spectrosc.* **1996**, *80*, 762.

(18) Hargittai, I.; Tremmel, J.; Kolonits, M. *HIS Hung. Sci. Instrum.* **1980**, *50*, 31.

(19) Tremmel, J.; Hargittai, I. *J. Phys. E* **1985**, *18*, 148.

(20) Wilson, A. J. C., Ed. *International Tables for X-ray Crystallography*, C; Kluwer: Dordrecht, 1995.

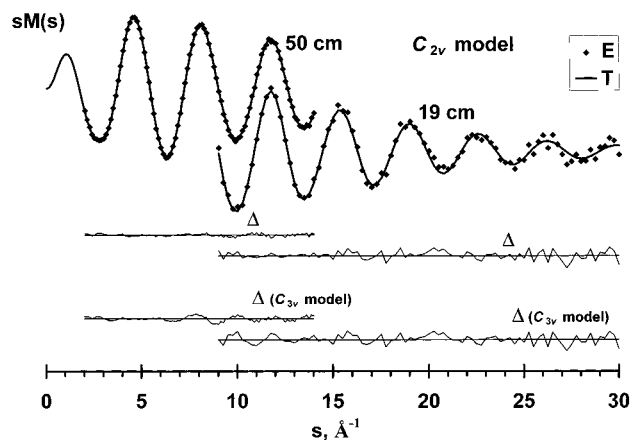


Figure 2. Experimental molecular intensities (E) of MnF_3 together with the calculated model for the C_{2v} geometry (T) and their difference (Δ). Difference curves for the C_{3v} -symmetry model are also indicated.

footing, single-reference calculations are unreliable. In the first part of our theoretical study we therefore surveyed many different geometrical arrangements of both triplet and quintet MnF_3 using CASSCF techniques and the MOLCAS program.²¹ In the initial phase we correlated 6 electrons in 8 orbitals, to give 108 CSF. The selection criteria were based upon the populations of the natural orbitals obtained from an MCPF calculation. Gradient methods were applied to locate stationary points on the quintet surface. Pseudopotential techniques were adopted for both Mn and F atoms; seven valence electrons were treated explicitly for fluorine and fifteen for (neutral) manganese, *i.e.* the 3s and 3p orbitals were included in the "valence" region. The Gaussian bases were of double- ζ quality for fluorine,²² augmented with diffuse p-type functions (4s, 5p contracted to 2s, 3p) and approximately triple- ζ quality for manganese,²³ augmented with a set of f-type polarization functions (8s, 7p, 6d, 1f, contracted to 6s, 5p, 3d, 1f).

Three different planar C_{2v} quintet states were located, with A_1 , B_1 and B_2 symmetries. Their geometries differ chiefly in the bond angles; there are two "small" angles of 106° in the 5A_1 state and two "large" angles of 128° in the 5B_2 species, while in the 5B_1 case all angles are fairly close to 120° (we adopt the convention where the molecule is located in the yz plane). The 5A_1 state is the lowest of these, being 25.7 kJ/mol below the 5B_2 species and 173 kJ/mol more stable than the 5B_1 state. Further CASSCF calculations were then performed, using a larger active space (8 electrons in 10 orbitals, to give 2000 CSF) and the geometries already located; the 5A_1 state remained the most stable, but its margin compared to the 5B_2 species diminished substantially, to only 10 kJ/mol. When dynamic correlation effects were also included by the CASPT2 method, the energy gap between these two states was reduced even further, to just 6.4 kJ/mol, though it is important to note that the relative ordering was not affected. No stationary point of C_{3v} symmetry could be found with use of CASSCF methods. While the bond lengths in the two lowest-lying quintet states are similar, with a total variation of some 0.04 Å, there are important systematic differences. In the 5A_1 state, we find two "long" and one "short" bond, whereas the pattern is reversed for the 5B_2 species (see also Figure 1). This distribution is

(21) MOLCAS3; Andersson, K.; Blomley, M. R. A.; Fülscher, M. P.; Karlström, G.; Kellö, V.; Lindh, R.; Malmquist, P.-Å.; Noga, J.; Olsen, J.; Roos, B. O.; Sadlej, A. J.; Siegbahn, P. E. M.; Urban, M.; Widmark, P.-O. University of Lund: Sweden.

(22) Bergner, A.; Dolg, M.; Küchle, W.; Stoll, H.; Preuss, H. *Mol. Phys.* **1993**, *80*, 1431.

(23) Dolg, M.; Wedig, U.; Stoll, H.; Preuss, H. *J. Chem. Phys.* **1987**, *86*, 866.

exactly what one would expect for two states linked by a Jahn–Teller distortion; depending on the phase adopted for the in-plane e' motion starting from a D_{3h} reference geometry, predominantly a bending vibration, one will obtain either one opened bond angle coupled with two lengthened bonds or two opened angles combined with one lengthened bond.

Four different triplet states were characterized, one of each possible symmetry with a C_{2v} planar geometry. The 3B_1 state was found to be the most stable triplet, followed in order by 3A_2 , 3A_1 , and 3B_2 . Geometry optimization was performed for the 3B_1 state only. Using the 6-electron CAS, these states are 280, 358, 366, and 485 kJ/mol less stable than the 5A_1 ground state, respectively. These results show unequivocally that all possible triplet states are substantially higher in energy than the lowest quintet. As the geometry of the ground state is the main focus of interest in the present work, no further work was performed on the triplet species.

In the second phase of the computational study we concentrated our attention on the calculation of the vibrational frequencies and force fields for the two low-lying 5A_1 and 5B_2 states. The CAS calculations showed, as expected, that a single configuration dominates in both of these species; the weight of the HF-reference configuration always exceeded 99%. We therefore adopted SCF and DFT methods for these vibrational frequency calculations, since they are less computationally demanding than the CASSCF variety. The Gaussian92 program was employed,²⁴ and standard all-electron basis sets were adopted for both fluorine and manganese atoms. The fluorine basis is a TZ contraction of Huzinaga's 10s, 6p primitives,²⁵ augmented with diffuse s and p functions (exponents 0.10 and 0.07, respectively) and a set of d-type polarization functions (exponent 0.8), to give a final contracted basis of [5 + 1s, 3 + 1p, 1d] quality. The s and p functions for Mn were taken from Wachters' 14s, 9p set,²⁶ flexibly contracted to 8s, 6p and augmented with a more diffuse p-type function (exponent 0.15). The (6/3) triple- ζ d set was taken from the work of Goddard and co-workers.²⁷ An f-type polarization function (exponent 0.6) was also added. The spherical-harmonic representation of both d-type and f-type functions was adopted. The "finergrid" option was used for numerical integration in the DFT calculations.

Geometries optimized for the two low-lying quintet states of C_{2v} symmetry are presented in Table 1. Absolute energies and energy differences between the two main quintet states are also reported. Several different methods were used, to assess the variability of the results obtained. Unrestricted HF and DFT techniques²⁸ were adopted, since these enable the second derivatives of the energy to be obtained analytically. Spin contamination was negligible, with $\langle S^2 \rangle$ values never exceeding 6.03. Excitations out of the eight lowest-energy MOs and into their virtual counterparts were excluded in the MP2 calculations; this choice of active space includes the 3s- and 3p-like manganese orbitals, in an attempt to incorporate at least part of any core-valence correlation effects. It is important to note that the angular parameters do not vary significantly with

(24) Gaussian 92-DFT: Frisch, M. J.; Trucks, G. W.; Head-Gordon, M.; Gill, M. W.; Wong, M. W.; Foresman, J. B.; Johnson, B. G.; Schlegel, H. B.; Robb, M. A.; Replogle, E. S.; Gomperts, R.; Andres, J. L.; Raghavachari, K.; Binkley, J. S.; Gonzalez, C.; Martin, R. L.; Fox, D. J.; DeFrees, D. J.; Baker, J.; Stewart, J. J. P.; Pople, J. A. Gaussian, Inc.: Pittsburgh, PA, 1992.

(25) Dunning, T. H. *J. Chem. Phys.* **1971**, *55*, 716.

(26) Wachters, A. J. H. *J. Chem. Phys.* **1970**, *52*, 1033.

(27) Rappe, A. K.; Smedley, T. A.; Goddard, W. A. *J. Phys. Chem.* **1981**, *85*, 2607.

(28) Becke, A. D. *J. Chem. Phys.* **1993**, *98*, 1372 and 5648. Lee, C.; Yang, W.; Parr, R. G. *Phys. Rev. B* **1988**, *37*, 785. Becke, A. D. *Phys. Rev.* **1988**, *A38*, 3098. Perdew, J. P. *Phys. Rev. B* **1986**, *33*, 8822.

Table 1. Geometrical Parameters and Energies Optimized for the ⁵A₁ and ⁵B₂ States of MnF₃^a

method	⁵ A ₁				⁵ B ₂			
	r(Mn ₁ -F ₂)	r(Mn ₁ -F ₃)	∠F ₂ -Mn ₁ -F ₃	-E ^b	r(Mn ₁ -F ₂)	r(Mn ₁ -F ₃)	∠F ₂ -Mn ₁ -F ₃	ΔE ^c
SCF	1.734	1.749	107.4	8.30211	1.774	1.734	127.5	8.7
B3LYP	1.734	1.755	106.6	10.77197	1.770	1.741	128.4	7.7
BLYP	1.752	1.775	106.9	10.80039	1.781	1.760	128.4	5.8
BP86	1.739	1.763	106.6	10.92030	1.771	1.747	128.8	6.4
MP2	1.726	1.752	105.7	9.21236	1.773	1.731	129.1	8.9

^a Distances in Å, angles in deg. For numbering of atoms see Figure 1. ^b Absolute energy, in hartree (au), below -1440 au. ^c Energy separation between ⁵A₁ and ⁵B₂ states, in kJ/mol.

Table 2. Harmonic Vibrational Wavenumbers and Calculated Infrared Intensities for MnF₃

normal mode	wavenumbers, cm ⁻¹						
	IR(Kr) ref 17	IR(Ar) ^a ref 17	Ra(Ar) ref 17	IR(Ne) ref 17	gas (estimated)	computed ^b	
						SCF	B3LYP
b ₂	752	759		774	778	811 (313)	788 (260)
a ₁	705	712		728	732	757 (166)	749 (129)
a ₁		644	644		660	695 (28)	666 (9)
b ₁	182	182	182	185	186	210 (104)	181 (58)
a ₁	186	186			190	194 (45)	180 (21)
b ₂					180	205 (8)	173 (3)

^a Experimental relative intensities: I₇₅₉:I₇₁₂:I₁₈₂ = 1:0.5:0.5, I₇₅₉:I₆₄₄ = 1:0.05-0.1, I₁₈₂:I₁₈₆ = 1:0.5. ^b Computed intensities, in parentheses, in km/mol.

method, and the differences between the two types of bond length for a given electronic state vary within a rather narrow range. Correlation effects on the bond lengths are small, of the order of the differences between the values obtained by the various methods.

Harmonic vibrational frequencies were calculated for the ⁵A₁ and ⁵B₂ states of MnF₃. There is now sufficient experience of DFT methods to suggest that they are likely to provide more reliable vibrational frequencies than either SCF or MP2 techniques,²⁹ so MP2 values were not obtained. There is one imaginary vibrational frequency (b₂ symmetry, an in-plane bending motion) predicted for the ⁵B₂ state at both SCF and B3LYP levels of theory. As the magnitude of this frequency is similar for both types of calculation (203i and 160i for SCF and B3LYP, respectively), it seems most unlikely that more sophisticated calculations would give results which are qualitatively different. Thus, it is clear that this ⁵B₂ species is the transition state on the pathway that links two equivalent ⁵A₁ states; the C_s motion "downhill" from the ⁵B₂ TS to the ⁵A₁ true minimum was followed at the SCF level for confirmation. The computed harmonic vibrational frequencies for the ⁵A₁ true minimum structure at the DFT level are given in Table 2.

Assignment of the Experimental Vibrational Spectra

Bukhmarina and Predtechenskii¹⁷ reported the vibrational spectrum of MnF₃ recorded in different inert gas matrices. Their most detailed spectrum is the IR spectrum recorded in Ar, but there are also some data from the IR spectra in Ne and Kr, and a Raman spectrum recorded in Ar.

The results are consistent with a distortion from D_{3h} symmetry. For this model there should only be three bands observed in the IR: the asymmetric stretch, the in-plane bend, and the out-of-plane deformation. However, four, or possibly five, bands were observed in the most detailed Ar matrix spectrum. The authors concluded that the molecule does not have D_{3h} symmetry, nor C_{3v} symmetry, and that the molecule is, probably, characterized by Jahn-Teller distortion. However, they did not give an assignment to their spectra.

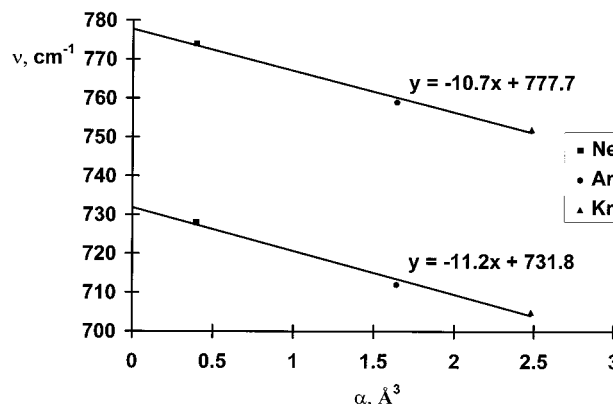


Figure 3. Estimation of the gas-phase vibrational wavenumbers of MnF₃ from the experimental wavenumbers measured in different matrices. The measured data are from ref 17.

Since we obtained the vibrational wavenumbers from our quantum chemical calculations, it was of obvious interest to match them with the experimental data of ref 17. Table 2 lists the relevant data together with the computed infrared intensities.

The assignment of the stretching wavenumbers is straightforward. There also seems to be a matrix shift that increases with the increasing polarizability of the noble gas. It has been suggested that the gas-phase wavenumbers can be predicted from the measurements in different matrices by extrapolation to zero polarizability. We did this extrapolation for the two largest wavenumbers and it gives a nice linear relationship indeed, as shown by Figure 3. Since we might suppose that the shift would be the same or at least similar for the symmetric stretch as well, we used the same equation to predict its gas-phase value.

There is only one experimental wavenumber for the deformation region (182 cm⁻¹) with possibly another, appearing as a shoulder on the more intensive peak (at 186 cm⁻¹), although Bukhmarina and Predtechenskii suggest that this shoulder is merely the consequence of matrix effect. On the basis of the comparison of experimental and computed infrared intensities, we suggest that the measured 182 cm⁻¹ band corresponds to the b₁ symmetry out-of-plane deformation mode.

The three computed deformation modes are very close to each

(29) See, for example: Hertwig, R. H.; Koch, W. J. *Comput. Chem.* **1995**, 16, 576. Ricca, A.; Bauschlicher, C. W. *Theor. Chim. Acta* **1995**, 92, 123. Ventura, O. N.; Kieninger, M. *Chem. Phys. Lett.* **1995**, 245, 488.

Table 3. Symmetry Coordinates for the Ground-State Geometry of MnF_3^a

$S_1(A_1) = \Delta r_{1,2}$
$S_2(A_1) = 2^{-1/2}(\Delta r_{1,3} + \Delta r_{1,4})$
$S_3(A_1) = 6^{-1/2}(2\alpha_{4,1,3} - \alpha_{2,1,4} - \alpha_{3,1,2})$
$S_4(B_2) = 2^{-1/2}(-\Delta r_{1,3} + \Delta r_{1,4})$
$S_5(B_2) = 2^{-1/2}(\alpha_{2,1,4} - \alpha_{3,1,2})$
$S_6(B_1) = \beta_{1,2,3,4}$

^a For numbering of atoms see Figure 1.

other. This suggests that the measured shoulder in the infrared spectrum may not be a matrix effect but, rather, a real wavenumber. Again, based on the infrared intensities, this could correspond to the a_1 vibration mode. Although their values are reversed in the calculation, this is only by 1 cm^{-1} , which is well within error limits. The third deformation mode, of b_2 symmetry, is of extremely low intensity from the computation, so this is also consistent with it remaining unobserved in the experiment.

One problem remains here, namely, the estimation of the gas-phase value of the b_1 frequency from the measured data. There does not seem to be a matrix shift for this mode, at least not between the Ar and Kr matrices, but there is a slight shift for the Ne matrix (see Table 2). Assuming this effect to be real, we can, again, estimate the gas-phase value at about 186 cm^{-1} . Accordingly, the value of the shoulder, at 186 cm^{-1} , should also be shifted somewhat, say, to 190 cm^{-1} .

On the basis of these five wavenumbers, the sixth can be estimated from the calculated values by using appropriate scaling. Thus we have a total set of estimated gas-phase wavenumbers for MnF_3 (see Table 2). It is notable that the values computed at the B3LYP level of theory agree well with these, without any need for scaling of any sort. Systematically, the stretching modes are overestimated by 1–2%, whereas the bending modes are slightly underestimated. The wavenumbers computed at the SCF level are decidedly less reliable, though the errors are still not large.

Normal Coordinate Analysis

Normal coordinate analyses were carried out for the C_{2v} distorted planar configuration of MnF_3 by using the program ASYM20³⁰ and the gas-phase wavenumbers estimated by us. These are given in Table 2. The molecule has six normal modes with the following irreducible representations:

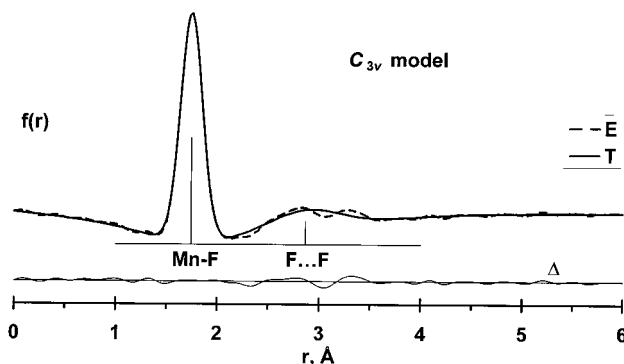
$$\Gamma_{\text{vib}} = 3a_1 + b_1 + 2b_2$$

The following internal coordinates were used to build up the symmetry coordinates (the numbering of atoms is given in Figure 1): Mn–F stretch ($\Delta r_{1,2}$, $\Delta r_{1,3}$, $\Delta r_{1,4}$), in-plane bend ($\alpha_{4,1,3}$, $\alpha_{2,1,4}$, $\alpha_{3,1,2}$), and out-of-plane bend ($\beta_{1,2,3,4}$). The symmetry coordinates are given in Table 3. The force field obtained from the B3LYP calculations was modified so as to reproduce the estimated gas-phase frequencies. The resulting force field is presented in Table 4. While it is of course not uniquely established as the harmonic force field for MnF_3 , we believe that it is unlikely to be significantly in error, as the discrepancies between the predicted and “experimental” (estimated gas-phase) wavenumbers are rather small.

The calculated parallel vibrational amplitudes were used as starting values in the electron diffraction analysis while the perpendicular vibrational amplitudes and the centrifugal corrections were used for transforming the electron diffraction distance parameters to r_α values.

Table 4. Elements of the Force Constant Matrix for MnF_3 (Stretching Force Constants in $\text{mdyn}/\text{\AA}$, Stretch–Bend Interactions in mdyn/rad , and Bending Force Constants in $\text{mdyn}\cdot\text{\AA}/\text{rad}^2$)

		1	2	3
A ₁	1	4.482		
	2	0.338	4.641	
	3	0.013	−0.006	0.289
B ₂	4		5	
	4	3.990		
	5	−0.167	0.323	
B ₁	6			
	6	0.083		

**Figure 4.** Experimental radial distribution curve (E) of MnF_3 with the calculated distribution of the C_{3v} model (T) and the difference curve (Δ).

Electron Diffraction Analysis

Figure 4 shows the experimental radial distribution curve of MnF_3 together with the calculated one for a C_{3v} model. Already this comparison shows that the molecule cannot have a pyramidal, or D_{3h} planar, geometry, which in both cases would be described by only two different kinds of distance, a Mn–F bond distance and a $F\cdots F$ nonbonded distance. The experimental radial distribution displays two well-resolved peaks in the $F\cdots F$ distance region, implying a model with two different $F\cdots F$ distances. This is in agreement with the proposed Jahn–Teller distortion of the molecule (see Figure 1) as well as with the computed minimum-energy geometry.

There are also two different kinds of Mn–F distance in the C_{2v} structure. These are, however, too close to each other and could not be resolved in the electron diffraction radial distribution. For this reason some constraints had to be introduced into the analysis.

First of all the difference between the two kinds of Mn–F distance was taken from the quantum chemical calculations and kept fixed. Depending on the level of the calculation this difference varied slightly, and this variation was taken into consideration in estimating the total errors of all parameters. As the best value we chose the MP2 results, giving $\Delta(\text{Mn–F}) = 0.026 \text{ \AA}$ with a conservative error limit of $\pm 0.020 \text{ \AA}$. The calculated vibrational amplitudes of the two Mn–F bond distances were used as starting values in the refinement and were varied with their difference unchanged.

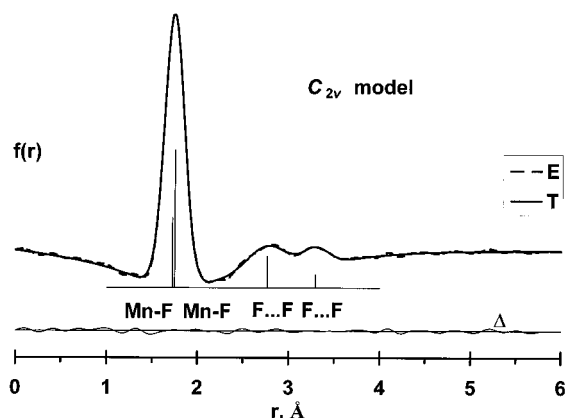
Another parameter that could not be varied simultaneously for both bond distances is their asymmetry parameter. With consideration of the results of different trial refinements as well as their values in similar molecules, such as FeF_3 ,¹² we decided to use a fixed value, corresponding to a Morse constant, $a = 2 \text{ \AA}$. The assumed value of the asymmetry parameter influences the bond lengths only. This was examined in separate trial refinements and was taken into consideration in estimating the total errors.

(30) Hedberg, L.; Mills, I. M. *J. Mol. Spectrosc.* **1993**, *160*, 117.

Table 5. Geometrical Parameters of MnF₃ from Electron Diffraction

parameter ^a	r_g representation	r_α representation	vibrational amplitude from NCA ^b
(Mn–F) _{ave} ^c	1.745 ± 0.004		
Δ(Mn–F) ^d	0.026		
$r(\text{Mn}_1\text{–F}_2)$	1.728 ± 0.014	1.712 ± 0.014	
$l(\text{Mn}_1\text{–F}_2)$	0.072 ± 0.003		0.058
$\kappa(\text{Mn}_1\text{–F}_2)$ ^e	8.8×10^{-6}		
$r(\text{Mn}_1\text{–F}_3)$	1.754 ± 0.008	1.735 ± 0.008	
$l(\text{Mn}_1\text{–F}_3)$	0.073 ± 0.003		0.060
$\kappa(\text{Mn}_1\text{–F}_3)$ ^e	9.5×10^{-6}		
$r(\text{F}_2\cdots\text{F}_3)$	2.771 ± 0.016		
$l(\text{F}_2\cdots\text{F}_3)$	0.199 ± 0.013		0.195
$r(\text{F}_3\cdots\text{F}_4)$	3.298 ± 0.017		
$l(\text{F}_3\cdots\text{F}_4)$	0.117 ± 0.012		0.118
$\angle_\alpha(\text{F}_2\text{–Mn}_1\text{–F}_3)$		106.4 ± 0.9	
$\angle_\alpha(\text{F}_3\text{–Mn}_1\text{–F}_4)$		143.3 ± 2.0	
R (%) ^f	6.25		

^a Distances in Å, angles in deg, asymmetry parameter in Å³. Indicated are total errors including twice the least-squares standard deviation, a 0.2% systematic error for distances and 2% for amplitudes, and the effect of constraints used in the analysis. ^b Mean-square vibrational amplitudes calculated by normal coordinate analysis based on estimated gas-phase vibrational frequencies of Table 2. ^c Average of Mn–F bond lengths. ^d Difference of Mn₁–F₂ and Mn₁–F₃ bond lengths (see Figure 1), used as a constraint and based on MP2 computations. ^e Asymmetry parameter fixed (see text). ^f Goodness of fit.

**Figure 5.** Experimental radial distribution (E) of MnF₃ with the calculated distribution of the C_{2v} distorted model (T) and the difference curve (Δ).

All other parameters could be refined simultaneously. The results of the electron diffraction analysis are given in Table 5. Figure 5 shows the radial distribution curve of the C_{2v} symmetry model together with the experimental distribution. The improvement in the agreement compared with that of the C_{3v} symmetry model is obvious.

Discussion

A gaseous MnF₃ molecule not exhibiting Jahn–Teller distortion would be expected to have a planar equilibrium geometry of D_{3h} symmetry. This, however, was already ruled out by the first electron diffraction study.¹⁵ Our observations have confirmed this, as a D_{3h} symmetry structure would imply unrealistically large, 0.15 Å, shrinkage effects, to approximate the experimental data. Such a large shrinkage would indicate a surprisingly small wavenumber of the out-of-plane vibration, or else the molecule should be described by a pyramidal equilibrium geometry. The latter, on the other hand, can be ruled out, based on the comparison with the C_{2v} model.

Comparison of the radial distribution curves of the C_{3v} and C_{2v} models in Figures 4 and 5 shows that the free MnF₃

molecule does, indeed, exhibit a Jahn–Teller-type distortion. The agreement between experimental intensities and the two models, expressed by the R factors (goodness of fit) is 6.3% and 9.8% for the C_{2v} and C_{3v} models, respectively. Moreover, the geometry of the C_{2v} model and the type of distortion leading to this structure is consistent with the prediction based on symmetry arguments on the one hand and with the results of the quantum chemical calculations on the other.

Some words about the previous electron diffraction study¹⁵ are also warranted here. Their inability to distinguish between the C_{3v} and the C_{2v} structures was a consequence of the lack of resolution of the two different F...F distances. The C_{3v} and C_{2v} models were approximating the experimental data to about the same extent (the corresponding R factors being 6.78% and 6.75%, respectively). Their reported bond lengths for the C_{2v} model, 1.733(25) and 1.743(13) Å, are in accordance with our results, considering their large uncertainty limits. However, the fact that the two distances were apparently refined simultaneously, with the calculated vibrational amplitudes constrained, and the asymmetry parameters ignored, precludes a reliable comparison of our results with those of ref 15.

Grichev et al. discuss the possible C_{2v} arrangement of MnF₃ based on the so called directional valencies,³¹ which is basically the same as the VSEPR model.³² They consider the central atom, manganese, having two lone electron pairs in addition to the three bonding pairs and assign a distorted trigonal bipyramidal electron domain geometry and, accordingly, a T-shape geometry to MnF₃. Typical molecules for this AX₃E₂ type are, for example, ClF₃³³ and BrF₃.³⁴ They have F_{ax}–A–F_{eq} bond angles somewhat smaller than 90° (87.5(2)° and 85(2)°, respectively), in keeping with the stronger repulsion from the two lone electron pairs positioning equatorially than from the bond to the equatorial fluorine atom. The C_{2v} structure of MnF₃ is not fully consistent with such a model. The bond angle that would correspond to F_{ax}–A–F_{eq} in MnF₃ is 106.4(0.9)°, that is the two axial fluorines bend in the direction towards rather than away from the supposed lone electron pair. Note also that the difference between the two types of bond lengths is much larger in ClF₃ and BrF₃ than in MnF₃ (0.102 and 0.081 Å vs 0.026 Å, respectively). Thus, rather than looking for a VSEPR-like explanation for the distortion of MnF₃ geometry, it seems to us straightforward to consider it the manifestation of the Jahn–Teller effect.

To compare the experimental geometry with the results of the computation, we have applied vibrational corrections to the experimental distances.³⁵ For this a normal coordinate analysis was carried out. The resulting average geometry is a so-called r_α -type representation, which differs from the equilibrium geometry only in the parallel anharmonic vibrational corrections. These r_α parameters consist of the distances between average nuclear positions and are also given in Table 5 together with the r_g thermal average distances. The computed bond lengths (Table 1) are equilibrium distances and should therefore be somewhat smaller than even the r_α values. In fact, they are all a little too large, with the MP2 results being the best, though the differences between the various theoretical values are mostly very small. On the other hand, it is particularly pleasing to note the remarkable agreement between the electron diffraction and computed values for the angular parameters: $\angle\text{F}_2\text{–Mn}_1\text{–}$

(31) Charkin, O. P. *Zh. Strukt. Khim.* **1969**, *10*, 754.

(32) Gillespie, R. J.; Hargittai, I. *The VSEPR Model of Molecular Geometry*, Allyn and Bacon: Boston, 1991.

(33) Haubrich, S. T.; Roerhig, M. A.; Kukolich, S. G. *J. Chem. Phys.* **1990**, *93*, 121.

(34) Ischenko, A. A.; Miakshin, I. N.; Romanov, G. V.; Spiridonov, V. P.; Sukhovkhov, V. F. *Dokl. Acad. Nauk SSSR (Engl)* **1982**, *267*, 994.

(35) Hargittai, M.; Hargittai, I. *Int. J. Quantum Chem.* **1992**, *44*, 1057.

F_3 is $106.4 \pm 0.9^\circ$ from electron diffraction and 106.6° from the B3LYP calculations. Here the MP2 level gives the worse agreement (105.7°), but even that angle is within the uncertainty of the experimental bond angle.

As to the precision of our experimental bond lengths, the average Mn–F bond distance is well-determined. The uncertainties assigned to the two individual bond lengths are large, reflecting our prudence in adopting a value for the difference between the two types of Mn–F bond length that was obtained by calculation. The ED experiment essentially contains no information on the value of that parameter, so a good fit to the ED data can be obtained with any value within rather large limits. The large uncertainty we have assigned to this difference is not an indication that the difference does not exist, it merely indicates the caution of treating constraints from other sources. There is little information available as to the reliability of calculated values for such small differences, precisely because they are so hard to determine from experiment. The uncertainty we have chosen is substantially larger than the range obtained by different methods of calculation, and it may indeed be too conservative.

The electronic populations on the manganese and fluorine atoms are of considerable chemical interest. At the SCF level we obtain a net charge on Mn of +1.61 e if the Mulliken method³⁶ is used, with $-0.53 e$ for the unique fluorine and $-0.54 e$ for the two equivalent F atoms. Virtually identical values are obtained from the CASSCF calculation, since the HF-reference configuration is so dominant. While the Mulliken method of population analysis is very widely used, it does have disadvantages when the basis contains diffuse functions, as here; it should be noted that diffuse functions are essential for molecules with a highly polar character. “Natural charges” have the advantage of being less sensitive to basis set than are the Mulliken variety.³⁷ For MnF_3 we find that the ionic character is more pronounced; the manganese net charge becomes +2.35 e, with $-0.76 e$ and $-0.80 e$ on the F atoms.

Although a species with strict D_{3h} symmetry does not appear to be a stationary point on the PE surface, its energy relative to the 5A_1 minimum is of obvious interest when considering the vibrational motion of MnF_3 . That geometry is 39.5 kJ/mol above the minimum if the CAS is considered, or 25 kJ/mol at the more complete CASPT2 level of theory. These differences are quite large compared to the barrier of about 7 kJ/mol, which separates equivalent 5A_1 minima. Our most reliable value of the calculated barrier height is probably the CASPT2 result of 6.4 kJ/mol. Fortunately, the SCF and B3LYP values are similar, at 8.7 and 7.7 kJ/mol, respectively, and the other DFT and MP2 results are also comparable (see Table 1). None of these values has been corrected for zero-point vibrational motion; such corrections are calculated to be of the order of 1.0 kJ/mol if the harmonic approximation is adopted. The potential surface may therefore be viewed as a “Mexican hat”, with three equivalent minima, each of C_{2v} symmetry with a different unique F atom along the C_2 axis. Each minimum will support several vibrational levels, as the bending quanta are of the order of 180 cm^{-1} or 2.2 kJ/mol.

At the high temperature (1000K) of the ED experiment kT is 8.3 kJ/mol so an appreciable fraction of the molecules will lie in vibrational levels above the barriers. Moreover, they will execute very large amplitude vibrational motion along the pathway linking two equivalent minima. We might also expect the vibrational motion along this 5A_1 – 5B_2 pathway to be strongly anharmonic. This all may explain why the experimental vibrational amplitudes differ somewhat from the calculated values. We have tried to incorporate transition-state molecules into our analysis, but the results were not sufficiently sensitive to their presence. The reason may be the relatively small contribution of the F···F distances to the electron scattering. Besides the signal/noise ratio for high-temperature data cannot be expected to be as favorable as is typically found for more routine experiments. Therefore, we did not judge it worthwhile to attempt to extract any information on the large-amplitude motion from the ED data.

It is interesting to see how similar the change in geometries appears in the crystal and gas-phase structures of first-row transition metal trifluorides. The two trifluorides next to MnF_3 , viz., CrF_3 and FeF_3 , exhibit high-symmetry geometries in both phases. They have undistorted, regular octahedral crystals with metal–fluorine distances of 1.90 and 1.92 Å in CrF_3 ³⁸ and FeF_3 ,³⁹ respectively. Their gas-phase geometry has D_{3h} symmetry and bond lengths of 1.732(2) (CrF₃ ref 11) and 1.763(4) Å (FeF₃ ref 12), respectively. The change in the metal–fluorine distance in both phases is in accord with the change in the d orbital occupation of the metal; the longest distance in the series can be expected for FeF_3 with the half-filled d-shell of iron.⁴⁰

Manganese trifluoride in between CrF_3 and FeF_3 , on the other hand, has a considerably distorted geometry in both phases. The crystals are monoclinic with two different shorter (1.817 and 1.912 Å) and one longer (2.088 Å) Mn–F distances,⁶ so the crystals are distorted from octahedral symmetry to close to D_{4h} . In the gas phase the distortion is also obvious—there is a C_{2v} symmetry geometry with two longer (1.754(8) Å) and one shorter (1.728(14) Å) Mn–F distance. In both the crystal phase and the gas phase the magnitudes of distortion are much beyond the experimental errors, so the effect is real. Due to the distorted molecular shape, the Mn–F distances are not comparable to the analogous distances of the other, symmetrical, trifluorides.

Acknowledgment. We are grateful to Dr. G. V. Girichev (Ivanovo, Russia) for sending us his experimental data on which the report of ref 15 was based. Although these data were not used in our final analysis, they stimulated us in carrying out a new electron diffraction experiment on manganese trifluoride. Part of this work was supported by the Hungarian Scientific Research Fund (Grant No. OTKA T 014073). C.J.M. thanks the IDRIS (Paris) for access to computing facilities. We thank Prof. Istvan Hargittai for advice. We appreciate the kind interest and encouragement of Dr. Edward Teller in this work.

JA9712128

(36) Mulliken, R. S. *J. Chem. Phys.* **1955**, *23*, 1833.

(37) Reed, A. E.; Weinstock, R. B.; Weinhold, F. *J. Chem. Phys.* **1985**, *83*, 735.

(38) Knox, K. *Acta Crystallogr.* **1960**, *13*, 507.

(39) Hepworth, M. A.; Jack, K. H.; Peacock, R. D.; Westland, G. J. *Acta Crystallogr.* **1957**, *10*, 63.

(40) Hargittai, M. *Inorg. Chim. Acta* **1991**, *180*, 5.